Nuclear Inst, and Methods in Physics Research B 426 (2018) 5–12

Contents lists available at ScienceDirect

Nuclear Inst. and Methods in Physics Research B

journal homepage: www.elsevier.com/locate/nimb

Computer simulation of sputtering induced by swift heavy ions

P. Kucharczyk*, A. Füngerlings, B. Weidtmann, A. Wucher

Fakultät für Physik, Universität-Duisburg-Essen, 47048 Duisburg, Germany

ARTICLE INFO

Keywords:
Sputtering
Sputtering yield
Angular distribution
Sputter statistics
Depth distribution
Energy distribution
Computer simulation

ABSTRACT

New experimental results regarding the mass and charge state distribution of material sputtered under irradiation with swift heavy ions suggest fundamental differences between the ejection mechanisms under electronic and nuclear sputtering conditions. In order to illustrate the difference, computer simulations based on molecular dynamics were performed to model the surface ejection process of atoms and molecules induced by a swift heavy ion track. In a first approach, the track is homogeneously energized by assigning a fixed energy to each atom with randomly oriented direction of motion within a cylinder of a given radius around the projectile ion trace. The remainder of the target crystal is assumed to be at rest, and the resulting lattice dynamics is followed by molecular dynamics. The resulting sputter yield is calculated as a function of track radius and energy and compared to corresponding experimental data in order to find realistic values for the effective deposited lattice energy density. The sputtered material is analyzed with respect to emission angle and energy as well as depth of origin. The results are compared to corresponding data from keV sputter simulations. As a second step of complexity, the homogeneous and monoenergetic lattice energization is replaced by a starting energy distribution described by a local lattice temperature. As a first attempt, the respective temperature is assumed constant within the track, and the results are compared with those obtained from monoenergetic energization with the same average energy per atom.

1. Introduction

The sputtering of atoms from a solid by ion bombardment is of great practical interest in areas related to the fabrication technology of semiconductor devices and to surface analysis techniques such as Secondary Ion Mass Spectroscopy (SIMS). In many applications, sputtering is induced by the impact of low energy ions with energies in the keV regime. In this case, the energy transfer between projectile and target is exclusively dominated by mostly elastic collisions, with the recoiling target atoms undergoing further collisions, and target atoms may be released from the surface at the end of such a collision cascade. In addition to the collisional "nuclear" energy loss $(dE/dx)_n$, the projectile experiences an electronic energy loss $(dE/dx)_e$ by generating electronic excitations within the target material. In the low energy regime, this electronic stopping has only a small influence on the particle ejection mechanism itself, but may influence the excitation or charge state of the sputtered particles [1,2].

At high impact energies, where a swift heavy ion impinges with a kinetic energy of the order of MeV/u, the situation changes. Here, the interaction with the nuclear system becomes negligible, and the slowing down of the projectile is caused almost solely by electronic stopping. Depending on the target material, the electronic excitation generated this way may rapidly spread and dissipate into the bulk of the irradiated sample without coupling to the atomic lattice. In other cases, the excitation stays localized around the trajectory of the incoming ion for a long enough time to efficiently couple energy into the lattice. In this scenario, electronic sputtering occurs if the lattice becomes energized enough to allow the evaporation of atoms. The sputter yield Y, i.e., the average number of atoms ejected from the surface per incident ion, observed for solids under such irradiation conditions is generally larger than would be expected from purely collisional sputtering [3].

To understand the energy exchange processes following the impact of a swift heavy ion, which ultimately lead to material modification and emission following the primary electronic excitation, thermodynamic models have been developed. These models are based on the assumption of a local thermal equilibrium described by a time and position dependent temperature both in the electronic and the lattice sub-systems of the solid. Moreover, it is assumed that the transport of energy within both systems is governed by diffusion. In the MeV/u energy range of interest here, the dominating energy transfer occurs via electronic stopping of the projectile, with the nuclear energy loss being negligible at these energies. The primary excitation generated in the electronic sub-system is rapidly shared and thermalized between the electrons on a femtosecond time scale, leading to an elevated electron

* Corresponding author.
E-mail address: pawel.kucharczyk@uni-due.de (P. Kucharczyk).

https://doi.org/10.1016/j.nimb.2018.04.002
Received 14 October 2017; Received in revised form 15 February 2018; Accepted 3 April 2018
Available online 22 April 2018
0168-583X/

temperature T_e, while the nuclear system is still at a low lattice temperature T_a and mainly heated via electron-phonon coupling. The spatio-temporal evolution of electron and lattice temperatures is then described by two coupled non-linear heat flow equations, leading to the generation of a thermal spike in the lattice sub-system. It is generally believed that track formation is observed when T_a exceeds the melting temperature of the material, whereas sputtering, i.e., the ejection of (sub-)surface material into the vacuum above the surface, occurs if the mean excitation energy per atom becomes comparable to the sublimation energy.

A thermodynamic description of particle emission from a thermal spike was published by Sigmund and Claussen [4]. Within this model, energy is assumed to be instantaneously deposited into the nuclear system within a cylindrical track volume centered around the trajectory of the impinging ion, producing a locally enhanced lattice temperature which spreads and dissipates according to the law of heat conduction in a continuum [5]. Particle emission is then described as the thermally activated evaporation from an ideal gas bounded by a planar surface barrier, where the evaporated flux is integrated over the spatio-temporal temperature distribution at the surface. In this work, the authors derived expressions for the total sputter yield as well as the emission energy distribution of the sputtered particles, with a central result being the prediction that the sputter yield should scale with the square of the initially deposited energy per unit track length. Assuming a constant conversion efficiency from electronic to lattice excitation energy, this would mean that the sputter yield should scale with $(dE/dx)_e^2$, a relation which has indeed been observed for fast ions incident on low-temperature condensed-gas solids [6]. A similar dependence is measured for insulators like oxides as well, while the yields measured for ionic crystals are generally found to increase more steeply [3]. For metallic samples, on the other hand, systematic investigations of this kind are still lacking.

A number of studies have been performed to test the concept of thermal spikes by using molecular dynamics (MD) to follow the nuclear motion within the target on a microscopic scale. As a result of such simulations, Bringa et al. [7] have shown that the assumption of a diffusive energy transport within the irradiated material is probably incorrect. Instead, they show that the particle motion is governed by a pressure pulse building up in the energized track region. Based on these results, Jakas et al. proposed a fluid dynamics approach to model the ejection process [8] in a way similar to the gas flow model published by Urbassek and Michl [9]. While the first simulations were performed on weakly bound systems using the pairwise additive Lennard-Jones potential to describe the interaction between the target atoms, it was later shown that the results were transferrable to metallic systems as well, provided the length and energies are scaled to the respective interatomic distances and binding energies [10]. Since these early studies involving an instant lattice energization as a starting point for the MD simulations, more sophisticated approaches have been developed where the time dependent nature of the local energy transfer to the lattice atoms is acknowledged. One possible approach is to employ a parametrized energy-time distribution derived, for instance, from a two temperature model (TTM) treating the energy coupling between electronic and nuclear subsystems. In order to further the details of the energy transfer processes, the TTM can be coupled to a Monte Carlo approach [11] describing the initial generation and redistribution of electronic excitation energy prior to electronic thermalization. Models of this kind have been successfully employed to describe structural modifications in insulators [12] and semiconductors [13,14]. Probably the most advanced simulations available today describing the interaction of a swift heavy ion with a solid combine a TTM-calculation of the electron temperature profile with an MD simulation which explicitly couples the atomic motion to the momentary electron temperature [15]. While models of this kind have successfully been applied to describe SHI-induced structural modifications [16], they have not yet been applied to electronic sputtering phenomena. An alternative concept to describe the lattice dynamics following the impact of a swift heavy ion is given by the Coulomb explosion model originally proposed by Fleischer et al. [17]. Within this model, target atoms along the ion trajectory become ionized by the projectile, and the resulting repulsion between the ionized atoms leads to track formation and particle emission. The dynamics as a consequence of an initially repulsive Coulomb force between the ionized atoms have also been followed by MD simulations and were shown to produce similar results as the thermal spike calculations [18].

In our group, we have recently started to perform sputtering experiments with swift heavy ions impinging onto various metal, semiconductor and insulator targets. In these experiments, we investigate the mass spectrum of secondary neutral and charged particles emitted from the bombarded surface due to the projectile ion impact. While the secondary ions are directly detected using a Time-of-Flight (ToF) spectrometer, neutral particles are post-ionized using a pulsed VUV laser beam to render them accessible for mass spectrometric analysis. In order to facilitate a quantitative comparison of secondary ion and neutral sputter yields, particular emphasis is put on the fact that both species are detected under otherwise identical experimental conditions regarding detection efficiency as well as the sampled solid angle and emission velocity intervals. Comparing the measured signal of post-ionized secondary neutral species with those of the corresponding secondary ions, it is possible to determine the ionization probability, i.e., the probability that a sputtered particle is emitted in a positively or negatively charged state.

One of the most interesting results of our studies is the fact that relatively large neutral sputter yields are observed for a few metallic targets irradiated by swift heavy ions with energies of about 5 MeV/u [19]. At these energies, amorphous tracks were previously found to form only in Ti and Zr [20]. These observations are notable, because metals are assumed to be insensitive to electronic energy-loss due to their high electron mobility. For the special case of a dynamically sputter cleaned polycrystalline indium sample being irradiated by 4.8 MeV/u gold ions, however, it was found that significant electronic sputtering of mostly neutral In atoms and In_n clusters occurs, with the ionization probability of the emitted indium atoms (leading to the formation of In^+ secondary ions) being about one order of magnitude larger than that determined in-situ under bombardment with 5 keV argon ions [21]. Moreover, the ionization probability measured under SHI impact was found to be practically insensitive of surface oxidation induced by deliberately exposing the sample to O_2. In contrast, secondary ion formation observed under keV argon ion bombardment exhibits the well-known oxygen matrix effect, leading to a drastic enhancement of the ionization probability by more than two orders of magnitude at the oxidized surface. From these experiments, it was concluded that the emission and ionization processes of sputtered particles must be fundamentally different under electronic and nuclear sputtering conditions, respectively. In particular, we suppose that the depth of origin of the sputtered particles must differ in a characteristic way, leading to the apparent insensitivity of electronically sputtered material to the chemistry of the uppermost surface layer.

In the present paper, we therefore model the emission process of (sub-) surface particles following a sudden energization of a certain lattice volume within a solid such as that generated by the impact of a swift heavy ion. The goal is to calculate the sputtering yield, i.e., the average number of atoms ejected from the solid, as a function of lattice excitation parameters such as the extension and energy content of the energized region. By comparing the resulting yield values with those observed in our experiments, we then determine “reasonable” excitation parameters, which are then used to calculate characteristics of the particle emission process such as the emission energy, angle and depth-of-origin distributions of the ejected particles. The resulting emission characteristics will then be compared with those prevailing under keV impact induced nuclear sputtering conditions in order to illustrate possible differences in the ejection mechanism under nuclear and

electronic sputtering conditions. As in the earlier studies by Bringa and others (see [22] for a review), we use molecular dynamics (MD) to follow the simultaneous motion of all target atoms, with the starting conditions being initialized in form of an energized cylinder oriented perpendicular to the solid surface. We chose silver as a model system for these calculations, since we have performed many MD simulations of nuclear sputtering events triggered by keV atom or cluster impacts for that system before. The results, however, should be transferable to the sputtering of indium as well, since the surface binding energies of indium and silver atoms (approximated by the respective sublimation energies of 2.6 and 3.0 eV) are comparable.

2. Numerical calculations

Classical MD simulations were performed using LAMMPS [23,24], a freely available open source molecular dynamics code. As a model sample, an (fcc)- crystal with an (1 0 0)-oriented surface was used, with the interaction of all target atoms being described by the many-body EAM-potential [25] fitted to the properties of solid silver. The cut-off radius r_{cut} of the potential was chosen as $r_{cut} = 5.55$ Å. As a starting condition for the MD simulations, atoms within a cylindrical volume of radius r_{cyl} around the projectile trajectory were assigned an initial kinetic energy, while all remaining crystal atoms were assumed to be initially at rest. In the context of an electronic sputtering szenario, this geometry would correspond to the impact of a swift heavy ion under normal incidence onto the crystal surface, which would penetrate the entire model crystal of about 10 nm thickness with only a small energy loss, thereby generating an energized "track" centered around its trajectory. Therefore, the excitation energy density within the track volume was assumed to be constant along cylinder axis throughout the entire crystal. In this context, we note that the "sudden energization" of the track volume as used here constitutes an oversimplification of the complex energy transfer processes following the impact of a swift heavy ion, since the spatio-temporal structure of the lattice energization is neglected. As already mentioned in the introduction, more sophisticated MD approaches exist where the lattice dynamics is connected with the projectile-induced electronic excitation using a two-temperature model [15]. In this so-called 2T-MD model, the atomic motion is coupled to the local electron temperature using a modified Langevin thermostat, while energy transfer back from the lattice to the electron subsystem is included in the MD simulation via an electronic friction force. While this approach delivers a more realistic description of the energy transfer from the electrons to the lattice, we do not expect a large influence of the energization mechanism on the particle dynamics following the initial excitation. For the purpose of the present paper, we therefore chose to stick with the sudden energization approximation for simplicity, since we are mainly interested in describing the particle emission process *following* the lattice excitation rather than the complex energy transport processes *causing* it.

Open boundary conditions were used at all surfaces of the model crystal, so that sputtering occurred as a consequence of the cylindrical lattice energization at both the top and the bottom surface simultaneously. It should be noted that the energy transport out of the side walls of the simulation cell is ignored this way. A proper treatment of the resulting cooling process would require an adaption of the MD energy distribution calculated *within* the simulation cell to that predicted by the heat diffusion equation in the undisturbed crystal *outside* the simulation cell, as discussed in detail elsewhere [26].* We have refrained from such a treatment here and investigated the possible influence of the lattice cooling effect by changing the size of the model crystal. As a result, we found no statistically relevant change of the calculated sputter yields when doubling the crystal size, indicating that the lattice cooling via energy transport out of the simulated crystal cell is negligible on the time scale investigated here. The simulations were then run until no more sputtering was detected or a maximum simulation time limit of 20 ps was reached.

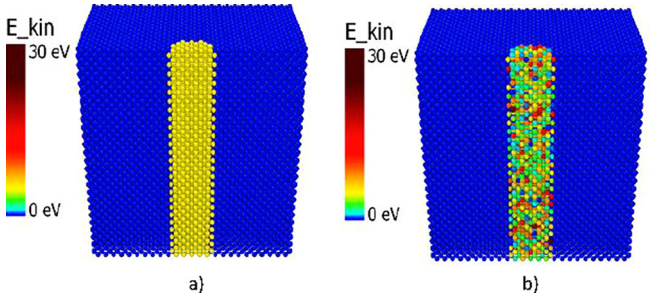

Fig. 1. Initial starting configurations of the MD simulations: (a) initial system with monoenergetic track atoms with $E_a = 5$ eV; (b) Maxwell-Boltzmann distributed initial energies of track atoms, described by local temperature T_a corresponding to the same average energy E_a per atom.

In order to identify the influence of the starting conditions, we varied the track radius r_{cyl} as well as the initial kinetic energy E_a of the atoms within the track. More specifically, for a fixed radius r_{cyl} the values $E_a = 3/4/5/6$ eV were used, while for a given E_a the track radius r_{cyl} was assumed as 1/1.5/2/2.5/3 times the lattice constant g (4.09 Å for silver). For each configuration, 20 simulations were performed, in which the major part of the sputtering process was identified to take place mostly during the first 3 ps. The sputtered atoms left behind a crater that reached its maximum depth at around 4 ps after the start of the simulation and began to fill up to a smaller depth again during the following picoseconds.

Energization of the atoms within the cylindrical track volume was initialized in two ways:

1. In a first approach, illustrated in Fig. 1a, all atoms within the track volume were assigned a fixed initial energy E_a, with the corresponding velocity vector $\overrightarrow{v_a}$ being randomly oriented in space.
2. In a second step of complexity, all atoms within the track were initialized by energies E_a^i, which were randomly chosen according to a Maxwell-Boltzmann (MB) probability distribution $f(v)$ described by a fixed local lattice temperature T_a. An example of such an initialization is shown in Fig. 1b.

The sample size used in each simulation depended on the total excitation energy and the radius of the track cylinder, ranging from $61.35 \times 61.35 \times 81.8$ Å^3 (19700 atoms) for $r_{cyl} = 4.09$ Å and $E_a = 3$ eV/atom up to $134.97 \times 134.97 \times 122.7$ Å^3 (136914 atoms) for $r_{cyl} = 12.27$ Å and $E_a = 6$ eV/atom. The crystal thickness, i.e., its dimension along the projectile ion track, was chosen in such a way that for all times the vertical distance between the craters formed at the upper and lower surface remained greater than approximately one crater depth (though the total thickness was never chosen smaller than 15 lattice constants, even for very shallow craters). This ensures that the limited thickness a many-particle MD simulation can handle did not affect the sputtering process. Since there is no distinguished vertical direction in these simulations, this allows to treat the sputtering from the upper and lower surfaces as equivalent and thus to obtain two statistically independent emission events per single simulation.

LAMMPS is a general-purpose MD simulation program and does not calculate sputtering yields per se. In order to identify sputtered particles, every 40 fs an output-file containing coordinates, velocity and energy of every atom was written. With our chosen simulation settings, LAMMPS discards atoms that move outside of it's so called simulation box, the sides of which were chosen as being 5 lattice constants away from the initial crystal's side faces. Atoms discarded this way were counted as sputtered if their properties during the previous timestep

* Note that the use of periodic boundary conditions is not appropriate here due to the localized nature of the excitation generated by a swift heavy ion impact.

fulfilled the following conditions:

1. The atom's vertical coordinate was above (respective below) the crystal's initial upper (respective lower) surface,
2. The atom's velocity had a vertical component directed away from the original surface,
3. The potential energy of the atom was either zero or small enough that the atom could not return to the crystal any more.

The results of the track emission simulations were compared to simulations of keV impacts onto a (111) oriented surface of a silver single crystal consisting of 4591 atoms, which were performed using the SPUT93 code with the Ag–Ag interaction being described by the MD/MC-CEM potential. Since these calculations have been described in great detail elsewhere [27,28], the procedures used to set up the system and to identify sputtered particles will not be described here. In these simulations, self sputtering conditions were employed using either single Ag atoms or Ag_n clusters as projectiles, so that the same many-body potential surface could be used to describe the interaction of all atoms in the entire system, and open boundary conditions were used at all sides of the model crystal as well.

3. Results

The goal of this work is to describe the emission characteristics of particles sputtered from an energized track following, for instance, the impact of a swift heavy ion. In particular, we wish to i) estimate the degree of lattice excitation which is necessary to produce experimentally observed sputter yields and ii) investigate the characteristics of the particle emission process following such an energization, particularly in view of the emission energy and angle distribution of the sputtered particles. The outcome of such simulations critically rests on two input parameters, namely the initial track radius and the (average) energy assigned to the atoms within the track. As a first step, we therefore vary both parameters and calculate the resulting total sputter yield, i.e., the average number of atoms removed from the crystal per projectile impact. In this context, we note that each simulation involves a random selection of starting velocities and therefore represents a statistically independent result of two sputtering events at the top and bottom surface of the model crystal, respectively. As a second step, we then select starting conditions leading to a realistic sputter yield and determine the resulting emission velocity and angle distribution of the sputtered particles. The results are compared with theoretical predictions as well as those obtained under keV ion impact induced collisional sputtering conditions. Particularly the latter is important in order to elucidate possible differences in the average emission velocity of the sputtered particles, which in turn are critical for the interpretation of experimental mass spectrometric data of sputtered particles as described below. As a third step, we then determine the depth-of-origin distribution of the sputtered material, with the goal to identify the possible influence of surface contamination on the average ionization probability of an emitted atom.

3.1. Sputter yield

The total sputter yield obtained from the MD simulations is shown in Fig. 2. Looking at the data, it should be kept in mind that the calculated numbers are only meant to identify parameter pairs E_a and r_{cyl}, which lead to reasonable, i.e., experimentally measured sputter yields. More specifically, the emission model presented here is not intended to *predict* or *explain* these parameters as a consequence of a specific SHI impact on a specific target material, since such a prediction would ultimately require a proper description of the complex energy transfer processes leading to the assumed lattice excitation.

The first obvious notice in Fig. 2 is that there is no significant difference in the sputter yields induced by a monoenergetic track initialization compared to those calculated for a quasi-thermal Maxwell-Boltzmann distribution of individual atom energies, as long as the average energy E_a per atom remains the same. As shown in the right hand side panel of Fig. 2, the relative difference between both starting conditions exhibits a statistical scatter around an average value of about 8%, which is overlayed by an apparent systematic trend towards higher deviation at lower values of the track radius r_{cyl}. We attribute this scatter to the statistics of the initial energy distribution in the quasi-thermal initialization, the relative significance of which must grow with decreasing track radius due to the decreasing total number of energized atoms.

Fig. 3 shows the correlation between the calculated sputter yield and the total lattice excitation energy

$$E_{total} = \pi r_{cyl}^2 E_a n_a \quad (1)$$

deposited in the system per unit track length. Here, n_a denotes the atom density of the target, which for the specific case of a silver target is 58.5 atoms/nm^3. It is seen from the log-log plot in Fig. 3 that the calculated sputter yield is roughly proportional to the square of the total lattice excitation energy assumed at the start of the simulation, a finding which is in principle predicted by the thermal spike model [29]. In fact, the Sigmund-Claussen model predicts the total lattice excitation energy to scale with the electronic energy loss $(dE/dx)_e$ of the projectile, leading to a predicted $(dE/dx)_e^2$ dependence of the sputter yield which has indeed been experimentally observed for some insulating targets such as oxides [3]. On the other hand, the total lattice excitation

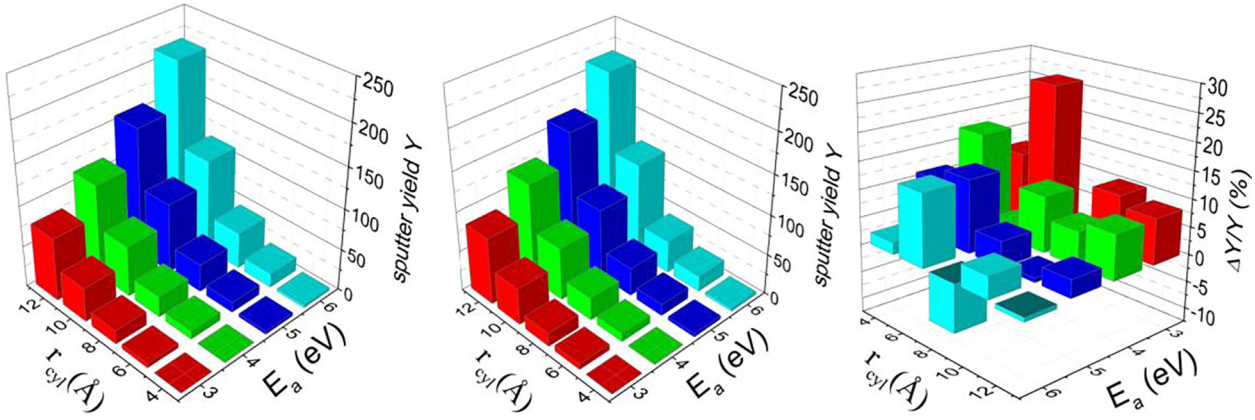

Fig. 2. Total sputter yield Y calculated for different values of the track radius r_{cyl} and the initial energy per atom E_a. Left panel: monoenergetic energization; middle panel: Maxwell-Boltzmann distributed initial energies at a temperature corresponding to the same average energy per atom; right panel: relative difference between both initial conditions.

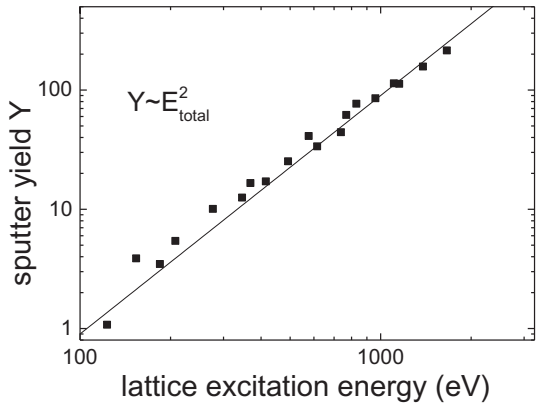

Fig. 3. Correlation of calculated sputter yield with total energy deposited in the track per unit length.

energy used here, leading to realistic sputter yields of $Y < 100$ atoms, is much smaller than the typical electronic energy loss experienced by the projectiles used in our experimental work. Calculating the electronic stopping power of a 5 MeV/u Au^{26+} projectile penetrating a metallic target like silver using the CASP† code [30], one finds a $(dE/dx)_e$ value of about 34 keV/nm. If this value was inserted as the starting lattice excitation energy here, this would correspond to very large energies E_a of the order of several hundred eV/atom, leading to unrealistically high calculated sputter yields. For the metallic targets investigated here, the results therefore illustrate the well-known fact that – due to the rapid transport of electronic excitation into the bulk of the target material – only a small fraction (~1%) of the electronically deposited energy actually ends up in the lattice system and is available for sputtering. We note, however, that the E_a values inserted here are significantly larger than those calculated from purely nuclear energy loss (0.6 eV/atom for the Au projectile mentioned above), thereby demonstrating that the electronically deposited energy is indeed needed in order to produce any sizeable sputter yield.

Using MD simulations similar to the ones obtained here, Bringa et al. have found a linear relation between track energy and sputter yields for high values of $(dE/dx)_e$, contradicting the thermal spike prediction, while they found a steeper dependence in the limit of low electronic energy loss [31]. As a criterion separating both regimes, they proposed to compare the deposited energy per atom with the sublimation energy U of the target material [8]. Comparing the respective value for silver (U = 3.0 eV) with the E_a values used here, one finds that our calculations reside in the transition region closely above that criterion, where the steep threshold behavior found in Ref. [8] gradually changes towards the linear dependence observed at higher excitation energies. Based on these facts, we note that our finding of a quadratic dependence may be fortuitous.

3.2. Yield statistics

The statistical distribution of sputter yields calculated for the same starting conditions with $r_{cyl} = 1$ nm and $E_a = 5$ eV/atom are shown Fig. 4 for a monoenergetic or Maxwell-Boltzmann distribution of the initial energies. Note that even for a fixed energy per atom the outcome is not deterministic, since the direction of the starting velocity vector is randomly selected for each energized atom. It is seen that the yield distributions calculated for monoenergetic and Maxwell-Boltzmann distributed initial energies show no significant difference, indicating that the nature of the sputtering process is essentially determined by the average energy per atom in the track. Compared to the keV simulations in the nuclear sputtering regime, the relative width of the distributions is narrower, with a standard deviation of about 13–16% as compared to 46% for the collisional sputtering process. Moreover, the average sputter yield of 13.6 atoms per keV ion impact is significantly smaller than that generated by the energized track. This finding is interesting since the range of the impinging 5-keV projectiles – as calculated by SRIM [32] – is of the order of 3 nm, so that the total energy deposited in the surface-near region relevant for sputtering amounts to about 1.6 keV/nm. Comparing this value with the energy deposited in the energized track, which for the example depicted in Fig. 4 amounts to about 1 keV/nm, one finds that both energy densities are comparable. This finding indicates that the lattice energy generated by a keV impact induced collision cascade is less effective for sputtering than a random track energization following, for instance, a swift heavy ion impact.

A possible reason for the relatively large scatter of the keV data is that – due to the single crystalline nature of the target – a channeling effect [33] might in principle occur during keV ion bombardment. If the projectile impact occurs along a low index crystallographic orientation, which is the case for normal incidence on the (1 1 1 surface), it may penetrate deeply into the target without depositing much of its energy in close proximity to the surface, where it can lead to sputtering. For certain favorable impact points, such a channeling event may therefore lead to exceptionally low sputtering yields, thereby contributing to the spread of the yield distribution. In the case of an initially energized track volume, on the other hand, the crystallographic order of the target atoms is of less importance.

3.3. Emission energy distribution

The angle integrated energy distribution of sputtered atoms following a monoenergetic and Maxwell-Boltzmann track energization with the same parameters r_{cyl} and E_a are very similar. As a typical result, Fig. 5 shows the energy distribution calculated for $r_{cyl} = 10.2$ Å and $E_a = 5$ eV/atom (full symbols). For comparison, the distribution obtained for 5-keV ion impact is included as well (open symbols). It is seen that the keV-induced nuclear sputtering process leads to a significantly broader emission energy distribution, which, however, does not quite fit the well-known cascade prediction [34]:

$$\frac{dY}{dE} \propto \frac{E}{(E+U)^3} \tag{2}$$

While the most probable emission energy is observed at U/2 – as predicted by Eq. (2), the decay towards larger energies calculated in the MD simulation appears to be steeper.

The energy spectrum calculated for the energized track volume can be compared to the prediction of the thermal spike emission model. For that purpose, we insert the track energy density of 1 keV/nm as the parameter F_D' into the formalism published by Sigmund and Claussen [4] and calculate the thermal emission yield Y_{th} and the emission energy spectrum according to Eqs. (9) and (14) of their paper. Using the track radius r_{cyl} as the initial core radius ρ_0 in their formalism, one obtains an initial core temperature $T_0 \sim 3 \times 10^4$ K, leading to $Y_{th} = 27.6$ atoms/track. Note that this value is by a factor 3 smaller than the MD result, indicating that the thermal spike model obviously underestimates the emission yield. The emission energy spectrum predicted by this model, however, appears to fit the calculated distribution remarkably well, as indicated by the solid blue line in Fig. 5. It is seen that the most probable emission energy expected for electronic sputtering under the track energization conditions depicted in Fig. 5 amounts to $E_{max} \sim 1.2$ eV, corresponding almost exactly to the Maxwell-Boltzmann prediction of $E_{max} = ½ kT_0$.

3.4. Emission angle distribution

The polar angle distribution of the emitted particles with respect to the surface normal shows no qualitative difference between

† The calculations were done using, UCA“ model and ‚charge state scan“ screening function

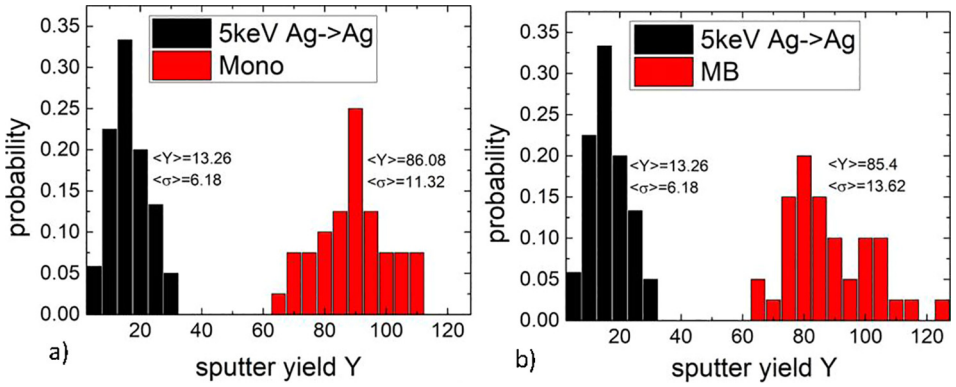

Fig. 4. Statistical distribution of sputter yields calculated for the same starting conditions with r_{cyl} = 1 nm and initial energies E_a = 5 eV/atom (red bars). In panel a), a monoenergetic initialization was used, whereas a Maxwell-Boltzmann distribution of initial energies with the same average energy was initialized in panel b). For comparison, the sputter yield statistics calculated for a 5 keV Ag atom impinging onto 120 different impact points uniformly distributed within the irreducible surface cell of an Ag(1 1 1) surface are included as black bars. (For interpretation of the references to colour in this figure legend, the reader is referred to the web version of this article.)

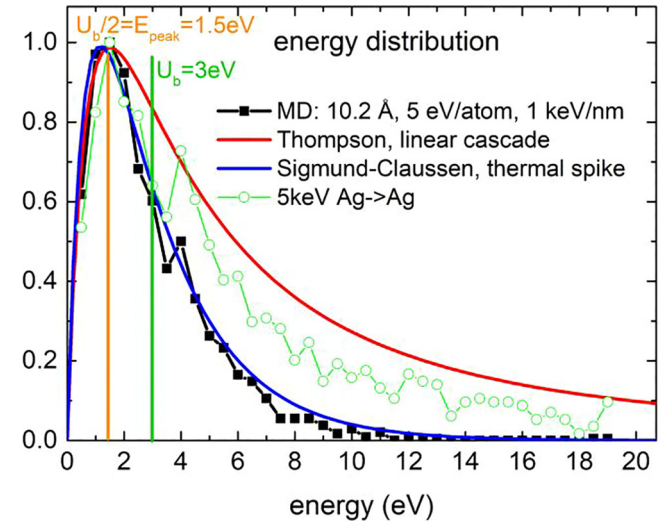

Fig. 5. Energy distribution of sputtered particles. Black dots: distribution calculated for monoenergetic track energization with track radius r_{cyl} = 1 nm and initial energy per atom E_a = 5 eV. Open symbols: energy distribution of sputtered atoms resulting from a 5 keV-Ag impact. Red curve: Thompson distribution predicted for linear cascade sputtering. Blue curve: prediction from Sigmund-Claussen thermal spike model. (For interpretation of the references to colour in this figure legend, the reader is referred to the web version of this article.)

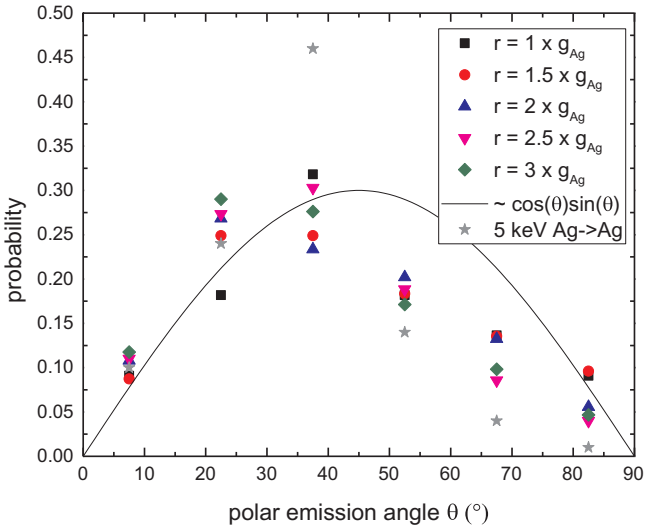

Fig. 6. Polar angle distribution of sputtered particles with respect to the surface normal as calculated for monoenergetic track energization at E_a = 4 eV. Solid line: sin(θ) * (cos(θ) dependence predicted by the Knudsen formula. The grey stars indicate the 5 keV Ag → Ag simulations.

monoenergetic and thermal track energization. As an example, we present the results integrated over the azimuth angle and calculated for monoenergetic track initialization with E_a = 4 eV and different track radii in Fig. 6. For comparison, the Knudsen distribution according to $f(\theta) \propto \cos(\theta)$ expected for purely thermal emission is included in the figure as a solid line. It is obvious that the Knudsen distribution fails to describe the calculated results, indicating a strong difference between the emission process under electronic sputtering conditions and a thermal spike. In view of the fact that the track "temperature" of several 10^4 K is clearly above the critical temperature of the target material, this discrepancy is not surprising. More specifically, the thermal emission theory ignores the immense pressure that is generated if the material is suddenly heated to such high temperatures. As a result, we feel that the emission process should be more accurately described as a phase explosion or thermodynamic expansion rather than thermal evaporation. Of note is that the angular emission distribution calculated for keV impact-induced collisional sputtering, also shown in Fig. 6 for reference, cannot be described by either of those dependencies as well.

3.5. Depth-of-origin distribution

In view of our recent experiments concerning secondary ion

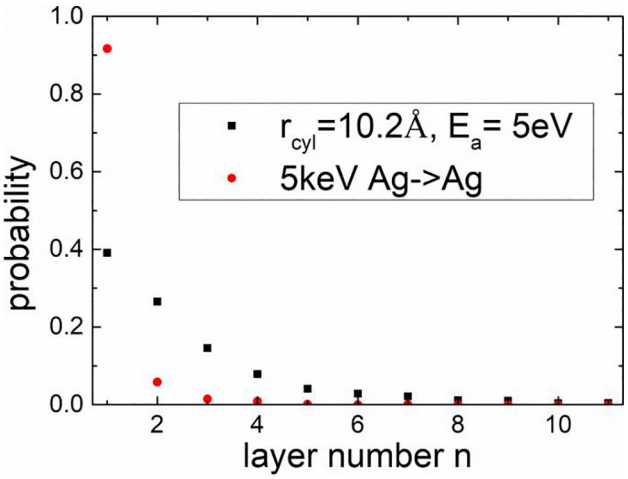

Fig. 7. Depth-of-origin distribution of sputtered atoms. Red bars: contribution of different atomic layers to the sputter yield calculated for track radius r = 2.5 g_{latt} = 1.023 nm and E_a = 5 eV, with the numbering of the layers such that the topmost surface layer being layer 1. Black bars represent the data resulting from simulations for a 5 keV-Ag-projectile impinging on a Ag(1 1 1)-surface and are shown for comparison. (For interpretation of the references to colour in this figure legend, the reader is referred to the web version of this article.)

Table 1
Connection between track radius r_{cyl} (in units of the lattice constant, here 4.09 A), total sputter yield Y and the contribution of the first layer to the sputter yield at constant energy per atom E_a = 4 eV.

Track radius	Track energy (eV/nm)	Sputter yield	1st layer contribution
1 g_{latt}	124	1.3	68%
1.5 g_{latt}	280	10.3	65%
2 g_{latt}	496	28.1	54%
2.5 g_{latt}	781	65.9	44%
3 g_{latt}	1116	123.78	37%

formation under swift heavy ion irradiation, it is of utmost interest to determine the depth of origin of the emitted particles. In particular, the finding of positive ionization probabilities of sputtered metal atoms which are practically independent of an oxygen surface coverage suggest that at least part of the emitted atoms must originate from deeper layers below the surface. In fact, the examination of this notion has been one of the main motivations for the present study, as outlined in the introduction.

As an example, the depth-of-origin distribution of sputtered atoms calculated for a track radius of about 1 nm and an initial energy of 5 eV/atom is shown in Fig. 7. For comparison, the corresponding distribution calculated for the impact of a 5 keV Ag atom is included. It is immediately evident that the two distributions exhibit a significant difference. The keV impact initiates a collision cascade, which leads to the emission of atoms originating mostly (92%) from the uppermost atomic layer. This result is typical for an emission event in the so-called linear cascade sputtering regime. In contrast, the emission mechanism triggered by the energized track leads to a much more pronounced contribution of deeper layers to the sputtered flux. In the simulation shown in Fig. 7, only 40% of the sputtered atoms originate from the uppermost atomic layer. As shown in Table 1, this contribution decreases with increasing track radius, provided the energy per atom is kept constant. In other words, the larger the sputter yield, the smaller the contribution of first layer atoms to the total flux of sputtered material.

This result explains why the nuclear sputtering process initiated by the keV projectile must be much more sensitive to surface contamination than that initiated by a MeV/u swift heavy ion impact. In the keV impact case, practically all emitted atoms have been in immediate contact with any contaminant covering the surface prior to their emission. For the particular case of an oxygen covered metal surface, the ionic character of the metal-oxygen bond leads to a strong enhancement of the probability for the emitted metal atoms to form a positive secondary ion once this bond is broken during the emission process. As a consequence, the ionization probability of sputtered metal atoms is found to increase by orders of magnitude once an originally clean metal surface becomes oxidized, a phenomenon that is well-known as the oxygen matrix effect in SIMS.

In contrast, many of the atoms emitted from an energized track never “see” the oxygen surface atoms during their emission process. As seen from the snapshots depicted in Fig. 8, the surface is quickly disrupted within a picosecond after the track energization. Practically all surface atoms are being ejected during this time, leaving behind a hot sub-surface volume where many particles are moving in a collective manner. Part of these atoms will later leave the solid and become sputtered, leaving behind a crater which is then gradually filled again during the recrystallization process following the particle emission. These atoms will not be influenced by any surface contamination pre-existing before the emission event, thereby explaining at least partly the experimental finding that their ionization probability is practically independent of the oxygen surface coverage.

4. Conclusion

Molecular dynamics simulations of (sub-)surface particle emission following the sudden energization of a cylindrical track are well suited to study the electronic sputtering process initiated by an impact of a swift heavy ion onto a solid surface. The calculated results indicate that there are no significant differences between monoenergetic or quasi-thermal track energization as long as the track radius and the average energy given to the track atoms remain unchanged. In particular,

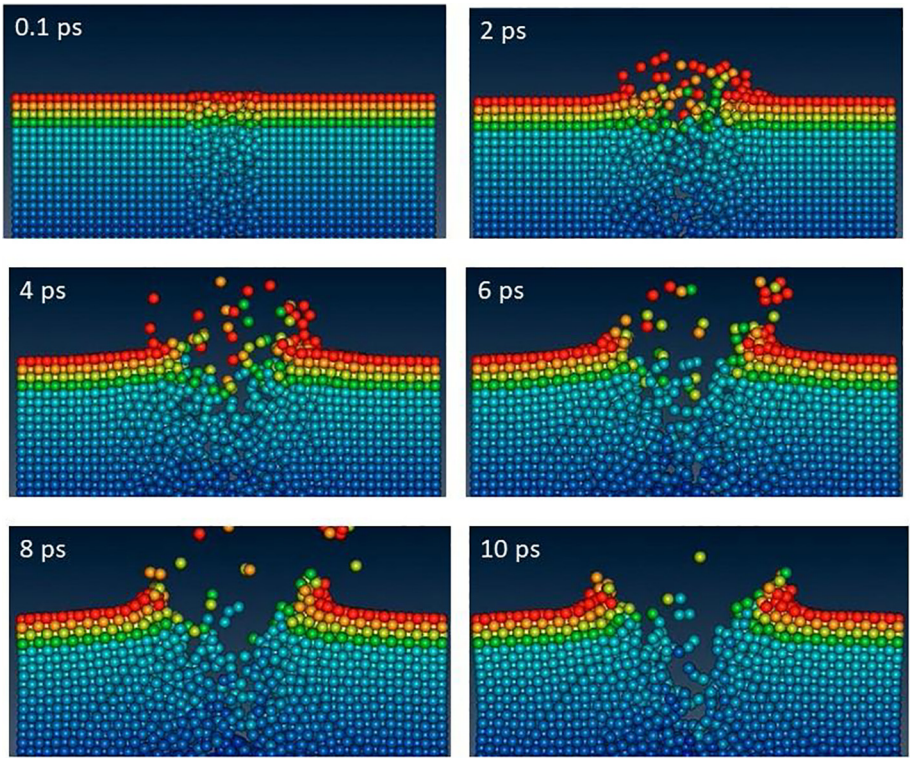

Fig. 8. Snapshots of the particle emission process from an energized track of radius r_{cyl} = 1 nm and energy E_a = 5 eV/atom.

neither the total sputter yield, its statistical variation nor the emission energy and angle distributions of the sputtered particles exhibit significant differences in that respect. While the emission energy distribution appears to be rather well described by the prediction of the Sigmund-Claussen thermal spike model, the calculated sputter yields are significantly larger than those predicted by this model. Moreover, the angular distribution of the emitted material reveals a clear deviation from the Knudsen prediction of a thermal spike, rather pointing towards a thermodynamic phase explosion of surface material induced by the sudden heating to overcritical temperatures and the accompanying pressure wave. These observations are in line with other hydrodynamic emission models published by other groups [8,9].

The depth-of-origin distribution of the sputtered material is found to substantially deviate from that found for typical nuclear sputtering in the linear cascade regime, as initiated, for instance, by the impact of a keV ion. The simulations clearly show that the relative contribution of first layer atoms residing at the outermost surface of the irradiated sample is significantly smaller under electronic sputtering conditions and decreases with greater track radius. These findings bear an important clue to the interpretation of recent experimental data on secondary ion formation at metallic surfaces irradiated by swift heavy ion projectiles. More specifically, they deliver at least partly an explanation for the stunning observation that the formation probability of positive secondary ions emitted under such irradiation conditions does not show the well-known oxygen matrix effect which is observed in keV impact induced Secondary Ion Mass Spectrometry (SIMS). It remains to be seen if other matrix effects commonly observed in SIMS can also be mitigated by using swift heavy ion projectiles as well.

Parallel to the simulations presented here, we are working on a more realistic approach to initialize the MD simulation. Due to the local nature of the initial energy deposition, it is unphysical to assume the same “temperature” or energy density within the entire track volume. For the sputtering applications targeted here, the symmetry of the track along the swift heavy ion trajectory appears reasonable and therefore will be kept in future work. In order to arrive at a more realistic temperature profile as a function of time and lateral distance from the track center, however, we plan to make use of the two-temperature approach to describe the heat exchange between electronic and nuclear dynamics in the same way as used in the inelastic thermal spike model [3]. The temperature evolution of the electronic and atomic subsystem will then be used to derive the lattice temperature profile $T_a(r,t)$ in order to initialize the MD simulations.

Acknowledgement

The authors gladly acknowledge financial support in the frame of the Collaborative Research Incentive (SFB) 1242 “Non-equilibrium dynamics of condensed matter in the time domain” and from the German Ministry of Science (BMBF) in the framework of the Verbundsprojekt 05K16PG1 “Ion Induced Materials Characterization and Modification”.

References

[1] A. Wucher, A. Duvenbeck, Kinetic excitation of metallic solids: progress towards a microscopic model, Nucl. Instr. Meth. B 269 (2011) 1655–1660.
[2] A. Wucher, B. Weidtmann, A. Duvenbeck, A microscopic view of secondary ion formation, Nucl. Instr. Meth. B 303 (2013) 108–111.
[3] W. Assmann, M. Toulemonde, C. Trautmann, Electronic sputtering with swift heavy ions, in: R. Behrisch, W. Eckstein (Eds.), Sputtering by Particle Bombardment, Springer, Berlin, 2007, pp. 401–450.
[4] P. Sigmund, C. Claussen, Sputtering from elastic-collision spikes in heavy-ion-bombarded metals, J. Appl. Phys. 52 (1981) 990–993.
[5] G.H. Vineyard, Thermal spikes and activated processes, Radiat. Eff. 29 (1976) 4.
[6] R.E. Johnson, L.J. Lanzerotti, W.L. Brown, Sputtering processes: erosion and chemical change, Adv. Space Res. 4 (1984) 41–51.
[7] E.M. Bringa, R.E. Johnson, L. Dutkiewicz, Molecular dynamics study of non-equilibrium energy transport from a cylindrical track. II. Spike models for sputtering yield, Nucl. Instr. Meth. B 152 (1999) 267–290.
[8] M. Jakas, E.M. Bringa, R.E. Johnson, Fluid dynamics calculation of sputtering from a cylindrical thermal spike, Phys. Rev. B 65 (2002) 165425–165429.
[9] H.M. Urbassek, J. Michl, A gas-flow model for the sputtering of condensed gases, Nucl. Instr. Meth. B 22 (1987) 480–490.
[10] O.J. Tucker, D.S. Ivanov, L.V. Zhigilei, R.E. Johnson, E.M. Bringa, Molecular dynamics simulation of sputtering from a cylindrical track: EAM versus pair potentials, Nucl. Instr. Meth. B 228 (2005) 163–169.
[11] N.A. Medvedev, A.E. Volkov, N.S. Shcheblanov, B. Rethfeld, Early stage of the electron kinetics in swift heavy ion tracks in dielectrics, Phys. Rev. B 82 (2010).
[12] O. Osmani, N. Medvedev, M. Schleberger, B. Rethfeld, Energy dissipation in dielectrics after swift heavy-ion impact: a hybrid model, Phys. Rev. B 84 (2011).
[13] T. Bierschenk, R. Giulian, B. Afra, M.D. Rodriguez, D. Schauries, S. Mudie, O.H. Pakarinen, F. Djurabekova, K. Nordlund, O. Osmani, N. Medvedev, B. Rethfeld, M.C. Ridgway, P. Kluth, Latent ion tracks in amorphous silicon, Phys. Rev. B 88 (2013).
[14] M.C. Ridgway, F. Djurabekova, K. Nordlund, Ion–solid interactions at the extremes of electronic energy loss: examples for amorphous semiconductors and embedded nanostructures, Curr. Opin. Solid State Mater. Sci. 19 (2015) 29–38.
[15] G.S. Khara, S.T. Murphy, S.L. Daraszewicz, D.M. Duffy, The influence of the electronic specific heat on swift heavy ion irradiation simulations of silicon, J. Phys. Condensed Matter 28 (2016).
[16] G.S. Khara, S.T. Murphy, D.M. Duffy, Dislocation loop formation by swift heavy ion irradiation of metals, J. Phys. Condensed Matter 29 (2017).
[17] R.L. Fleischer, P.B. Price, R.M. Walker, Ion Explosion spike mechanism for formation of charged-particle tracks in solids, J. Appl. Phys. 36 (1965) 3645–3652.
[18] E.M. Bringa, R.E. Johnson, Coulomb explosion and thermal spikes, Phys. Rev. Lett. 88 (2002) 165501.
[19] L. Breuer, P. Ernst, M. Herder, F. Meinerzhagen, M. Bender, D. Severin, A. Wucher, Mass spectrometric investigation of material sputtered under swift heavy ion bombardment, Nucl. Instr. Meth. B (2018).
[20] A. Barbu, A. Dunlop, D. Lesueur, R.S. Averback, Latent tracks do exist in metallic materials, EPL (Europhys. Lett.) 15 (1991) 37.
[21] M. Herder, P. Ernst, L. Breuer, M. Bender, D. Severin, A. Wucher, Secondary ion formation on indium under nuclear and electronic sputtering conditions, J. Vac. Sci. Technol. A (2018), http://dx.doi.org/10.1116/1.5018721.
[22] H.M. Urbassek, Sputter theory, Kgl. Dansk. Vid. Selsk. Mat. Fys. Medd. (2006) this.
[23] S. Plimpton, Fast parallel algorithms for short-range molecular dynamics, J. Comput. Phys. 117 (1995) 1–19.
[24] lammps.sandia.gov.
[25] M.S. Daw, M.I. Baskes, Embedded-atom method: derivation and application to impurities, surfaces, and other defects in metals, Phys. Rev. B 29 (1984) 6443–6453.
[26] A. Duvenbeck, A. Wucher, Low-energy electronic excitation in atomic collision cascades: a nonlinear transport model, Phys. Rev. B 72 (2005) 165408.
[27] M. Lindenblatt, R. Heinrich, A. Wucher, B.J. Garrison, Self-sputtering of silver by mono- and polyatomic projectiles: a molecular dynamics investigation, J. Chem. Phys. 115 (2001) 8643–8654.
[28] A. Wucher, B.J. Garrison, Cluster formation in sputtering: a molecular dynamics study using the MD/MC-corrected effective medium potential, J. Chem. Phys. 105 (1996) 5999–6007.
[29] E.M. Bringa, M. Jakas, R.E. Johnson, Spike models for sputtering: Effect of the surface and the material stiffness, Nucl. Instr. Meth. Phys. Res. Sect. B 164 (2000) 762–771.
[30] www.casp-program.org.
[31] E.M. Bringa, R.E. Johnson, M. Jakas, Molecular-dynamics simulations of electronic sputtering, Phys. Rev. B 60 (1999) 15107–15116.
[32] www.srim.org.
[33] D.S. Gemmell, Channeling and related effects in the motion of charged particles through crystals, Rev. Mod. Phys. 46 (1974) 129–227.
[34] M.W. Thompson, Atomic collision cascades in solids, Vacuum 66 (2002) 99–114.